Aspects of dynamic models of robots

Aspects of dynamic models of robots

H. H. van de Ven *

SUMMARY

This paper deals with some aspects of the dynamic behaviour of an industrial robot. First the kinematical problem involving coordinate transformation from fixed-world coordinates to robot coordinates is described. Next dynamic models are derived following the Lagrange and Newton Euler approaches. Some trends in robot technology are given. Further the concept of modelling a robot with one and two degrees of freedom as a mass-damper-spring system is described. The model includes the nonlinearities in the actuator systems.
The time response and the frequency response have been determined by means of a simulation program. By comparing the measurements with those of a real robot system it could be concluded that the arm of the robot cannot be modelled as a rigid body. From the parameter sensitivity analysis it was determined that the harmonic-drive parameters are the most important ones.

1. INTRODUCTION

Mechanical manipulators are already used for heavy and too hazardous or unpleasant human work in industrial environments for long periods of time. They can be used only for restricted and well-defined, specialized and preappointed tasks. These kinds of manipulators fall outside the classification of industrial robots. The Robot Institute of America developed for an industrial robot the following definition :

"A robot is a programmable, multi-function manipulator designed to move material, parts, tools or special devices through variable programmed motions for the performance of a variety of tasks".

Industrial robots have become increasingly important in industrial flexible automation in recent years. The industrial robots in current applications and future developments are divided into three generations. The great majority of present industrial robots (first generation) perform relatively simple repetitive tasks, such as elementary handling tasks, spot-welding and paint spraying in the automobile industry. Those robots are controlled so that the end-effector moves from point to point or along a particular path in a coordinate system that is fixed in relation to the environment. The controller possesses only internal feedback loops of motor positions and velocities. On account of the absence of sensors, the first generation robots do not react to uncertainties in the position of the end-effector and to changes in their environment and therefore the accuracy is limited. Derivations in the end-effector position and changes in environment conditions can only be corrected if the robots are able to observe their environment via sensors. Robots with sensors belong to the second generation. They are able to follow a continuous path through feedback of the information obtained from the sensor and after its processing in the control system. These robots can perform more accurate work such as electric-arc-welding and assembling.
By extending the robot system with capabilities of learning the task to be performed and processing the previous experiences in the control system, the robot can search for the optimal strategy. Therefore, the third generation robot must not only be equipped with sensors, but must also have a flexible pattern recognition system and a certain form of self-organization, in other words, equipped with artificial intelligence. These industrial robots are still in a state of development and are not yet found in an industrial environment.
As the performance requirements of robot systems are increased, their control systems are also becoming more advanced. For advanced control and design of robot systems, knowledge of the manipulator dynamics is essentially important. Thus the first step in the development of suitable control algorithms is the derivation of a dynamic model for the mechanical manipulator. Robot model building and simulation should be directed towards two main groups, robot system designers and the users.

2. CLASSICAL APPROACHES TO MANIPULATORS DYNAMICS

It is generally assumed that any mechanical manipulator can be considered to consist of several rigid bodies, called links or arms, connected in series by revolute or prismatic joints. One end of the open chain is attached to a supporting base, while the other end is free. The joints are

* Dept. of Electrical Engineering, Eindhoven University of Technology, POB 513, NL-5600 MB Eindhoven, The Netherlands.

driven by an actuator. When building a model of a manipulator, it is convenient to separate the overall model into a model of the arm mechanism and models of the actuator circuits.
For deriving the equations of motion of the arm mechanism, a fairly general approach is feasible. Suppose each joint-link pair constitutes one degree of freedom (d.o.f.). Hence an n-th d.o.f. manipulator contains n joint-link pairs. The joints and links are numbered outward from the base. The base of the manipulator is link 0 and is not considered to be a part of the robot. Joint 1 is the connection point between link 1 and the supporting base.
When modelling the mechanical structures of the robot, two aspects are of vital importance; the robot arm kinematics and dynamics. Kinematics deals with robot arm position with respect to a fixed-reference coordinate system as a function of time and is often referred to as the "geometry of motion". Dynamics deals with the mathematical formulations of the equations of robot arm motion. Differential equations are the most usual mathematical form.

2.1. Arm kinematics

The motion of rigid bodies may be described by using a fixed coordinate system or by using moving coordinate systems. The motion of the moving coordinate system is specified with respect to a fixed coordinate system. The fixed coordinate system in Newtonian mechanics is the primary inertial system which is assumed to have no motion in space. From an engineering point of view the fixed system may be taken as any system whose absolute motion is negligible for the problem at hand. This is why an inertial coordinate frame is usually established on the supporting base of the robot.
Since the robot links can rotate or translate with respect to a reference coordinate frame, an orthogonal coordinate system is assigned to each link. These frames rotate or translate with respect to each other. The kinematics problem is then reduced to find a transformation matrix that relates the moving frames in the links to the reference frame, that is to say mapping the robot's internal

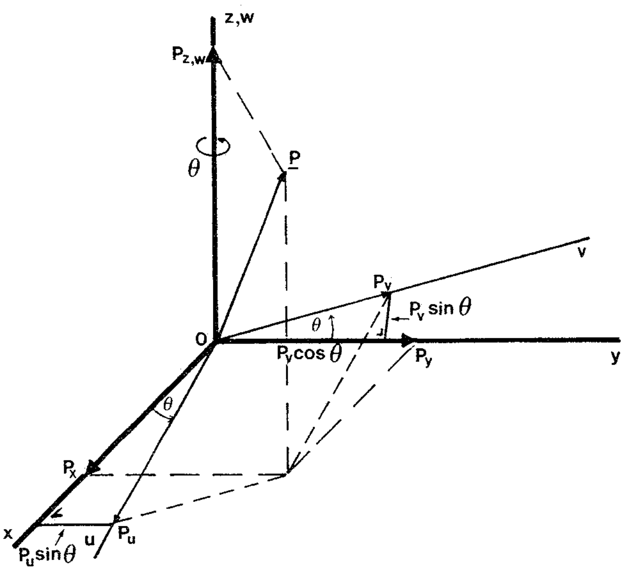

Fig. 1. Rectangular coordinate systems

coordinates to the external world's coordinates.
The relative rotations between two consecutive frames can be expressed by means of 3 x 3 rotation matrices. Figure 1 shows two rectangular systems, the frame-xyz is assumed to be fixed and the frame-uvw has arrived from a rotation θ around the z-axis of the reference frame. A position vector $\underline{p}$ in the moving frame-uvw can be represented by its components with respect to both coordinate systems.
From figure 1 the following relations can be derived :

$$p_x = p_u \cos\theta - p_v \sin\theta; \; p_y = p_u \sin\theta + p_v \cos\theta; \; p_z = p_w$$

In vector-matrix notation

$\underline{p}_{xyz} = R_{z,\theta}\, \underline{p}_{uvw}$ with the transformation matrix

$$R_{z,\theta} = \begin{bmatrix} \cos\theta & -\sin\theta & 0 \\ \sin\theta & \cos\theta & 0 \\ 0 & 0 & 1 \end{bmatrix}$$

The indices at $\underline{p}$ refer to the relevant coordinate system and the indices at R refer to the rotating axis and rotation angle.
Similarly rotation matrices for rotation around the x-axis with angle ϕ and around the y-axis with angle a, are respectively :

$$R_{x,\phi} = \begin{bmatrix} 1 & 0 & 0 \\ 0 & \cos\phi & -\sin\phi \\ 0 & \sin\phi & \cos\phi \end{bmatrix}; \; R_{y,a} = \begin{bmatrix} \cos a & 0 & \sin a \\ 0 & 1 & 0 \\ -\sin a & 0 & \cos a \end{bmatrix}$$

The rotation matrices are orthogonal.
Any finite rotation matrix can be found from these basic rotation matrices. The resultant rotation matrix R that represents a rotation of θ around the z axis, followed by a rotation of a around the (new) y-axis, followed by a rotation of ϕ around the (new) x-axis can be calculated from :

$$\underline{p}_{xyz} = R_{z\theta}\underline{p}_{uvw} = R_{z\theta} R_{ya} \underline{p}_{rst} = R_{z\theta}\, R_{ya}\, R_{x\phi} \underline{p}_{\ell mn} \text{ and}$$

$$R = R_{z\theta} R_{ya} R_{x\phi} = \begin{bmatrix} C\theta Ca & C\theta Sa S\phi - S\theta C\phi & C\theta Sa C\phi + S\theta S\phi \\ S\theta Ca & S\theta Sa S\phi + C\theta C\phi & S\theta Sa C\phi - C\theta S\phi \\ -Sa & Ca S\phi & Ca C\phi \end{bmatrix}$$

where C. = cos. and S. = sin.

The 3 x 3 rotation matrix does not present the facilities for translation and scaling. For that purpose homogeneous coordinates are introduced. In the homogeneous coordinate representation a three-dimensional position vector $\underline{p}^1 = (p_x\ p_y\ p_z)$ is represented by an augmented vector

$$\underline{p}^1 = (wp_x\ wp_y\ wp_z\ w) \text{ with } p_x = \frac{wp_x}{w}; \; p_y = \frac{wp_y}{w};$$

$p_z = \frac{wp_z}{w}$ and w = 0. $\underline{p}^1$ represents the transpose of $\underline{p}$. In robotics applications the scale factor w is always chosen equal to 1. In this concept a 4 x 4 homogeneous

transformation matrix maps a vector represented in homogeneous coordinates from one coordinate system to another.
Generally, the homogeneous transformation matrix H is composed as follows :

$$H = \left[\begin{array}{ccc|c} & R & & \underline{p} \\ \hline 0 & 0 & 0 & 1 \end{array}\right] \tag{1}$$

R is the already considered rotation matrix and $\underline{p}$ is the translating vector. The transformation matrix corresponding to a translation by a vector $\underline{p}^1 = (a\ b\ c)$ and a rotation ϕ around the x-axis are, respectively

$$H_{tr} = \begin{bmatrix} 1 & 0 & 0 & a \\ 0 & 1 & 0 & b \\ 0 & 0 & 1 & c \\ 0 & 0 & 0 & 1 \end{bmatrix} ; H_{x\phi} = \begin{bmatrix} 1 & 0 & 0 & 0 \\ 0 & \cos\phi & -\sin\phi & 0 \\ 0 & \sin\phi & \cos\phi & 0 \\ 0 & 0 & 0 & 1 \end{bmatrix}$$

A general expression of the transformation matrix H is :

$$H = \begin{bmatrix} n_x & s_x & a_x & p_x \\ n_y & s_y & a_y & p_y \\ n_z & s_z & a_z & p_z \\ 0 & 0 & 0 & 1 \end{bmatrix} = \begin{bmatrix} \underline{n} & \underline{s} & \underline{a} & \underline{p} \\ 0 & 0 & 0 & 0 \end{bmatrix} \tag{2}$$

The first column of H represents the coordinates of the new x-axis with respect to the reference frame. Similarly the second, third and fourth columns represent the coordinates of the y-axis, z-axis and the origin of the new frame with respect to the reference frame.
As indicated before, the manipulator is considered to consist of a series of links connected together by joints and there is one coordinate system assigned to each link. Using homogeneous transformation, the relative position and orientation between these coordinate frames are described. In attaching coordinates to each link, the Denavit and Hartenberg convention is mostly used (fig. 2).

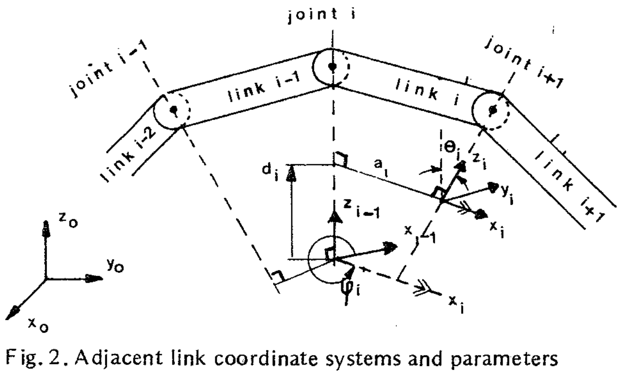

Fig. 2. Adjacent link coordinate systems and parameters

A base coordinate system $(x_0\ y_0\ z_0)$ is set as $-z_0$ is along the direction of gravity. The z_i-axis lies along the axis of motion of the joint i+1, the x_i-axis directs along the common normal from z_{i-1} to z_i-axis, and y_i-axis is chosen to complete the right coordinate system. The origin of the coordinate system of link i is set to be at the intersection of the common normal between the axes of joint i and i+1 and the axis of joint i+1.
Any link can be characterized by two quantities : the common normal distance a_i and the angle θ_i between the axes in a plane perpendicular to a_i. The joint axis will have two normals on it, one for each link. The relative position of two such connected links is given by d_i, the distance between the normals along the joint axis and the angle ϕ_i between the normals measured in a plane normal to the joint-axis.
Having assigned coordinate frames to all links according to the preceding scheme, we establish the relationship between successive frames i-1 and i by the following rotations and translations : (a) rotate around the z_{i-1}-axis by an angle ϕ_i; (b) translate along z_{i-1}-axis by a distance d_i; (c) translate along x_i-axis (rotated x_{i-1}), a length a_i; and (d) rotate around x_i-axis by the twist angle θ_i. The relations (a) to (d) can be expressed as a product of four homogeneous transformations relating the coordinate frame of link i to the coordinate frame of link i-1.

$$A_i^{i-1} = H_{z\phi_i} H_{tr,zd_i} H_{tr,xa_i} H_{x\theta_i} =$$

$$\begin{bmatrix} C\phi_i & -S\phi_i C\theta_i & S\phi_i C\theta_i & a_i C\phi_i \\ S\phi_i & C\phi_i C\theta_i & -C\phi_i S\theta_i & a_i S\phi_i \\ 0 & S\theta_i & C\theta_i & d_i \\ 0 & 0 & 0 & 1 \end{bmatrix}$$

The homogeneous transformation matrix T_i^j which specifies the position and orientation of link i with respect to the coordinate frame of link j, is the chain product of successive transformation matrices of A_i, expressed as :

$$T_i^j = A_{j+1}^j \, A_{j+2}^{j+1} \ldots\ldots A_i^{i-1} \quad \text{with } i > j$$

The joints can either be rotational or translational. If they are rotational, a_i, d_i and θ_i are constants and ϕ_i is variable. If they are translational, a_i, ϕ_i and θ_i are constants and d_i is variable. At on-line applications three of the four basic transformations in A_i^{i-1} can be calculated beforehand.
The inverse of a homogeneous transformation $[T_i^j]^{-1} = T_j^i$ specifies the position and orientation of link j with respect to the coordinate frame of link i.

$$T_j^i = \begin{bmatrix} n_x & n_y & n_z & -\underline{n}^1\underline{p} \\ s_x & s_y & s_z & -\underline{s}^1\underline{p} \\ a_x & a_y & a_z & -\underline{a}^1\underline{p} \\ 0 & 0 & 0 & 1 \end{bmatrix} \tag{4}$$

2.2. Arm dynamics

Various approaches are available for formulating robot arm dynamics such as Lagrange equations, Newton-Euler equations, d' Alembert's formalisms, bond graphs, Hamiltonian and virtual work formulation. In the literature the equations described by Lagrange and Newton-Euler are used most frequently. For systems with multiple d.o.f. it is generally convenient to choose coordinates, called generalized coordinates, q_i, which are independent of one another. Generalized coordinates may be lengths or angles or any other set of independent quantities which define the position of the system.

2.1.1. Lagrange equations

The dynamic model based on the method of Lagrangian generalized coordinates will be derived from the Lagrangian function $L = K-U$, where K is the kinetic energy of the system and U is the potential energy. The kinetic and potential energy of the system may be expressed in any convenient coordinate system.

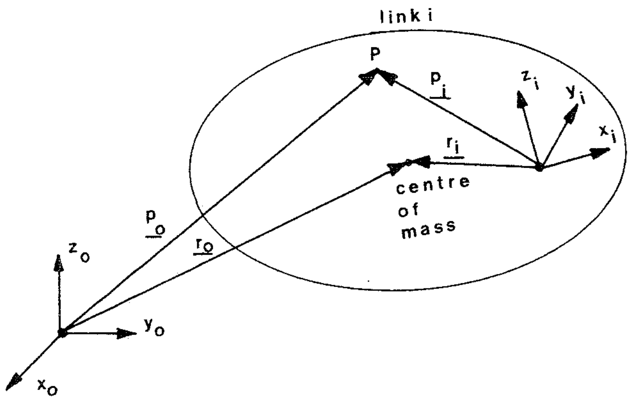

Fig. 3. Position of link i with respect to the base frame

Consider a point p on link i (fig. 3) whose position in coordinate frame i is given by $\underline{p}_i$. The position of point p with respect to the base frame is represented by $\underline{p}_0$. The transformation between these two frames is

$$\underline{p}_0 = T_i^0 \, \underline{p}_i \tag{5}$$

By differentiating equation (5) the absolute velocity of $\underline{p}_0$ is found. Now, the kinetic energy of link i is found by expressing the kinetic energy of a differential mass dm located at point p and integrating over the link

$$K_i = \frac{1}{2} \int_i \sum_{j=1}^{i} \sum_{k=1}^{i} \mathrm{Tr}\, \{\frac{\partial T_i^0}{\partial q_j} \dot{q}_j \, \underline{p}_i \, \underline{p}_i^1 \left[\frac{\delta T_i^0}{\partial q_k}\right]^1 \dot{q}_k \}dm$$

where Tr is the trace operator.
By summing over all n links, then the total energy of the robot arm with respect to the base frame is

$$K = \sum_{i=1}^{n} [\frac{1}{2} \mathrm{Tr}\, \{ \sum_{j=1}^{i} \sum_{k=1}^{i} \frac{\partial T_i^0}{\partial q_j} J_i \left[\frac{\partial T_i^0}{\partial q_k}\right]^1 \dot{q}_j \dot{q}_k \}] \tag{6}$$

where $J_i = \int_i \underline{p}_i \underline{p}_i^1 dm$ is the symmetric generalized inertia tensor of link i.
The potential energy of a link whose center of mass is described by a vector $\underline{r}_i$ with respect to i-th coordinate frame is $U_i = - m_i \underline{g}^1 \underline{r}_i$ where vector $\underline{g}$ represents the gravity row vector, $\underline{g}^1 = (g_x \, g_y \, g_z \, 0)$. The total potential energy of the robot arm with respect to the base frame is

$$U = \sum_{i=1}^{n} -m_i \underline{g}^1 T_i^0 \underline{r}_i \tag{7}$$

The Lagrangian function L can be formed from equations 6 and 7. The Euler-Lagrange equation 8 relates the generalized forces F_i to the generalized coordinates q_i

$$\frac{d}{dt} \frac{\partial L}{\partial \dot{q}_i} - \frac{\partial L}{\partial q_i} = F_i \tag{8}$$

Substituting the Lagrangian function into equation 8, we obtain

$$\sum_{j=1}^{n} B_{ij} \ddot{q}_j + \sum_{j=1}^{n} \sum_{k=1}^{n} C_{ijk} \dot{q}_j \dot{q}_k + D_i = F_i \tag{9}$$

for i = 1, 2, ..., n.
The coefficients in equation 9 are

$$B_{ij} = \sum_{p=\max(i,j)}^{n} \mathrm{Tr}\{\frac{\partial T_p^0}{q_j} J_p \left[\frac{\partial T_p^0}{\partial q_i}\right]^1 \};$$

$$C_{ijk} = \sum_{p=\max(i,j,k)}^{n} \mathrm{Tr}\{\frac{\partial^2 T_p^0}{\partial q_j \partial q_k} J_p \left[\frac{\partial T_p^0}{\partial q_i}\right]^1 \};$$

$$D_i = - \sum_{p=i}^{n} m_p \underline{g}^1 \frac{\partial T_p^0}{\partial q_i} \underline{r}_p$$

The physical meaning of these dynamic coefficients is : B_{ii} represents the effective inertia at joint i; B_{ij} represents coupling inertia between joint i and j; C_{ijj} relates centripetal forces at joint i due to velocity at joint j; C_{ijk} relates Coriolis forces at joint i due to velocities at joint j and k; D_i represents the gravity loading at joint i.
The linear inertial terms and the gravity terms are always important in robot control. The dynamic non-linear terms for the centripetal and coriolis forces are important only when the robot arm is moving at high speed.

2.2.2. Newton-Euler equations

There are a number of formulations of the equations of motion based on the Newton-Euler equations. As with the Lagrangian method a coordinate frame is attached to each link of the manipulator. This is done following the Denavit-Hartenberg convention. The relation between the coordinate frames of two successive links is described by a rotation matrix R and by a translation vector $\underline{p}$, which are expressed in equations 1 to 4. For manipulators having all rotary joint R_i^j $(j < i)$ specifies the position and orientation of link i with respect to the coordinate frame of link j, while $R_j^i = [R_i^j]^1$ specifies the position and orientation of link j with respect to the frame of link i.

The procedure in the Newton-Euler formulation is to write first the equations which describe the angular and linear velocities and accelerations of each link with respect to the own coordinate frame going from the base of the robot to the gripper (forward recurrence) and next calculate the forces and torques from the gripper back to the base of the robot (backward recurrence).

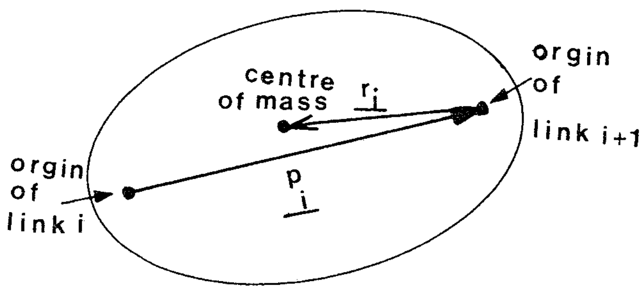

Fig. 4. Positions of origin and centre of mass of link i

Since, by the Denavit-Hartenberg convention an angular motion of link i is around the z_{i-1} axis, then for a rotational joint, the recursive Newton-Euler equations are (fig. 4) :

$$\underline{\omega}_i = R^i_{i-1} \; (\underline{\omega}_{i-1} + \underline{z}_{i-1}\dot{q}_i)$$

$$\underline{\dot{\omega}}_i = R^i_{i-1} \; \{\dot{\omega}_{i-1} + \underline{z}_{i-1} \ddot{q}_i + \underline{\omega}_{i-1} \times (\underline{z}_{i-1} \dot{q}_i) \}$$

$$\underline{\dot{v}}_i = \underline{\dot{\omega}}_i \times \underline{p}_i + \underline{\omega}_i \times (\underline{\omega}_i \times \underline{p}_i) + R^i_{i-1} \; \underline{\dot{v}}_{i-1}$$

$$\underline{\ddot{r}}_i = \underline{\omega}_i \times \underline{r}_i + \underline{\omega}_i \times (\underline{\omega}_i \times \underline{r}_i) + \underline{\dot{v}}_i$$

$$\underline{F}_i = m_i \underline{\ddot{r}}_i$$

$$\underline{N}_i = J_i \underline{\omega}_i + \underline{\omega}_i \times (J_i \underline{\omega}_i)$$

where

$\underline{\omega}_i$ = angular velocity of link i; $\underline{v}_i$ = linear velocity of link i;
$\underline{\ddot{r}}_i$ = acceleration of the centre of mass of link i;
m_i = mass of link i;
$\underline{F}_i$ = total force exerted on link i;
$\underline{N}_i$ = total moment exerted on link i;
J_i = constant inertia tensor of link i around its centre of mass and
x denotes the cross product

For the interaction force and moment yield

$$\underline{f}_i = \underline{F}_i + R^i_{i+1} \underline{f}_{i+1}$$

$$\underline{n}_i = R^i_{i+1} \, \underline{n}_{i+1} + \underline{p}_i \times (R^i_{i+1} \underline{f}_{i+1})$$
$$+ (\underline{p}_i + \underline{r}_i) \times \underline{F}_i + \underline{N}_i$$

where $\underline{f}_i$ and $\underline{n}_i$ are force and moment exerted on link i by link i-1, respectively.

The actuator torque τ_i exerted on link i is

$$\tau_i = \underline{n}_i^1 z_{i-1}$$

The recursive relations of velocities and accelerations between link i-1 and i are initialized to indicate a stationary base.

$\underline{\omega}_0 = \underline{0}; \underline{z}_0 = [0\ 0\ 1]^1, \underline{\dot{v}}_0 = [0\ 0\ g]^1$ with g is the gravitational acceleration. Note that $\underline{z}_{i-1} = R_0^{i-1} \, \underline{z}_0 = \underline{z}_0$.

A similar set of equations can be derived if the joint is translational.

3. UTILITY OF THE MODELS AND TRENDS ON MANIPULATOR PERFORMANCE

Generally speaking the two approaches of section 2 are equivalent. The Newton-Euler formulation by forward and backward recursive equations is compact and, in spite of "messy" vector cross product terms, the computation time of the applied torques or forces can be reduced to allow real-time control. However, because of its recursive computation, it does not provide much insight for deriving advanced control laws.

The Lagrange approach is simple and well-structured. This formulation can be expressed in matrix notation and is therefore attractive from a control point of view. But the highly non-linear dynamic equations of motion as formulated are usually computationally inefficient and real-time control has been difficult to achieve.

To improve the speed of computation, the most common method has been to simplify the dynamics by ignoring second order terms such as the Coriolis and centripetal forces. However, such an approximate model, when used in control, results in suboptimal dynamic performance, restricting arm movement to low speed. At fast speed of movement, the neglected terms become significant and make accurate position control of the robot arm impossible.

The accuracy is also affected by vibrations which can arise in not fully rigid bodies. Traditionally, structural vibration has been avoided by increasing the rigidity of the arm. Such an approach adds considerable mass to the robot, leading to higher material cost and higher total system weight, increased torque and power requirement to accelerate the mechanism. Such a manipulator is restricted to low speed of motion. However, the trend in manipulator design has been to continually improve performance by increasing both precision and speed of motion. This requires : on the one hand high-speed, light-weight manipulator configurations, and more advanced control systems for the actuators on the other hand.

In the interest of better arm design, one would like to understand the limitation imposed by the structure on arm performance. These limitations are strongly related to the type of control scheme used and can be reduced through appropriate design of the controller by recognizing the flexible nature of the arm structure. Thus, to ensure good performance, methods for the sys-

tem analysis and for the control system design are to be developed, which take the elastic properties of the light structures into account from the beginning.
In principle, the number of degrees of freedom of flexible mechanical systems is infinite, due to the distributed parameters. At the Eindhoven University of Technology, research has been going on into modelling flexible manipulator systems. Available research tools such as boundary element method, finite element method, structural analysis programs, model analysis and Fourier analysis techniques will be useful in this respect.
In optimising the dynamic performance of a robot, the behaviour of the actuator systems plays an important part. In modelling robot mechanism, little attention has been paid to the effects of the use of gear-boxes as torque-transmitting devices. Some motor gear-box combinations introduce torsional elasticity, non-linear friction and backlash, the effects of which have to be investigated. The quality of the physical and mathematical models of a robot are fundamental to the analytical development and physical interpretation of manipulator dynamics. Exclusion of dominant manipulator features can result in an over-simplified model. Thus, improvement of robot dynamic performance will depend on the availability of better dynamic models in order not only to improve the mechanical design according to its structural dynamics, but also to compensate for the unavoidable flexibility and nonlinearity effects through appropriate design of the controller.
Improved models of a robot are usually acquired at some cost. They lead to extensive sets of non-linear algebraic and differential equations. The solving of these equations requires a relatively high speed computer system with a large memory and much computation time. These models simply do not lend themselves to real-time applications in accordance with the present state of the art in computer technology, but they are essential for obtaining insight into the dynamic robot behaviour. They also provide the key to justified substantial reduction of the scope of the model. Apart from this, research is needed on improved algorithms, task-oriented and more powerful languages.

4.1. Improved model of a robot with one degree of freedom

An industrial robot is a positioning device in that each of its joints has a positional control system. This also holds for a robot with a single d.o.f. The control system consists of comparison units, a control unit, a d.c. servomotor with tachometer and resolver, gear-box (harmonic-drive) and load.

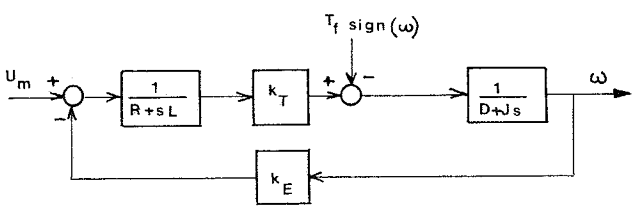

Fig. 5. Block diagram of the servomotor

The block diagram of the permanent magnet d.c. servomotor is shown in figure 5, where : L = inductance and R = resistance of the motor armature winding, respectively; K_T = torque constant; K_E = back electromotive force constant; J = motor inertia, D = viscous damping coefficient; T_f = a non-linear friction torque, due to coulomb friction which is constant but always opposite to the relative motion.
Another type of nonlinearity may be encountered such as stiction, which is the force required to initiate motion. In actual practice, the stiction force gradually decreases with velocity and changes over to coulomb friction at reasonably low speed.
The mechanical part of the control systems consists of the rotor of the motor, the rotor of the tachometer, the wave-generator in the harmonic-drive and the load. The relatively small inertia of the resolver is charged on the inertia of the tachometer.
A useful engineering description of the time response of mass systems is accomplished by the solution of a mathematical model of an equivalent system which can be readily analysed. A useful equivalent of the mechanical system is that of the concentrated mass mounted on an elastic spring and a dashpot representing the viscous damping.

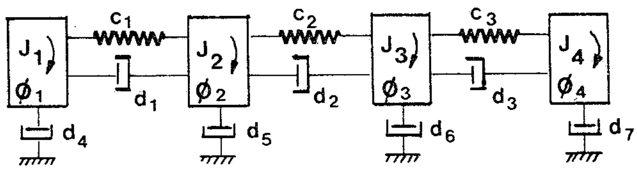

Fig. 6. A physical model of the mechanical system

Figure 6 shows a physical model of the mechanical parts of the system, where :
J_1, J_2 and J_3 are the inertias of the tachometer, motor and harmonic-drive, respectively; J_4 is the effective inertia due to the load and the gear ratio; d_4, d_5 and d_6 are viscous damping coefficients and d_7 is the effective damping coefficient; d_1, d_2 and d_3 represent the dissipation coefficients due to the twist of the shafts; c_1 and c_2 are stiffness coefficients and c_3 is the effective stiffness.
Φ_1, Φ_2, Φ_3 and Φ_4 are angular displacements. The motor torque is exerted on J_2.
The equations of motion can be derived with the extended Lagrange equation for systems with dissipative elements.

$$\frac{d}{dt}\left(\frac{\partial K}{\partial \dot{q}_i}\right)-\frac{\partial K}{\partial q_i}+\frac{\partial U}{\partial q_i}+\frac{\partial W}{\partial \dot{q}_i}=Q_i \tag{10}$$

where W represents the dissipated energy.
The generalized coordinate q_i can be chosen as ϕ_i. The only generalized torque Q_i is the torque T from the motor.
The kinetic energy can be written as

$$K=\frac{1}{2}\sum_{i=1}^{4} J_i\,\dot{\phi}_i^2 \tag{11}$$

The potential energy is the energy stored in the springs namely :

$$U = \frac{1}{2} \sum_{i=1}^{3} c_i (\phi_{i+1} - \phi_i)^2 \tag{12}$$

The dissipated energy is the energy lost by viscous friction

$$W = \frac{1}{2} \sum_{i=1}^{3} d_i(\dot\phi_{i+1} - \dot\phi_i)^2 + \frac{1}{2} \sum_{i=1}^{4} d_{i+3}\, \dot\phi_i^2 \tag{13}$$

Substituting equations 11, 12 and 13 into equation 10 yields for each coordinate equation

$$J_1 \ddot\Phi_1 = c_1(\Phi_2 - \Phi_1) + d_1 (\dot\Phi_2 - \dot\Phi_1) - d_4 \dot\Phi_1 \tag{14}$$

$$J_2 \ddot\Phi_2 = T + c_1 (\Phi_1 - \Phi_2) + d_1 (\dot\Phi_1 - \dot\Phi_2) - d_5 \dot\Phi_2 + c_2 (\Phi_3 - \Phi_2) + d_2 (\dot\Phi_3 - \dot\Phi_2) \tag{15}$$

$$J_3 \ddot\Phi_3 = c_2 (\Phi_2 - \Phi_3) + d_2 (\dot\Phi_2 - \dot\Phi_3) - d_6 \dot\Phi_3 + c_3 (\Phi_4 - \Phi_3) + d_3 (\dot\Phi_4 - \dot\Phi_3) \tag{16}$$

$$J_4 \ddot\Phi_4 = c_3 (\Phi_3 - \Phi_4) + d_3 (\dot\Phi_3 - \dot\Phi_4) - d_7 \dot\Phi_4 \tag{17}$$

Laplace transform of these equations leads to the block diagram of figure 7.

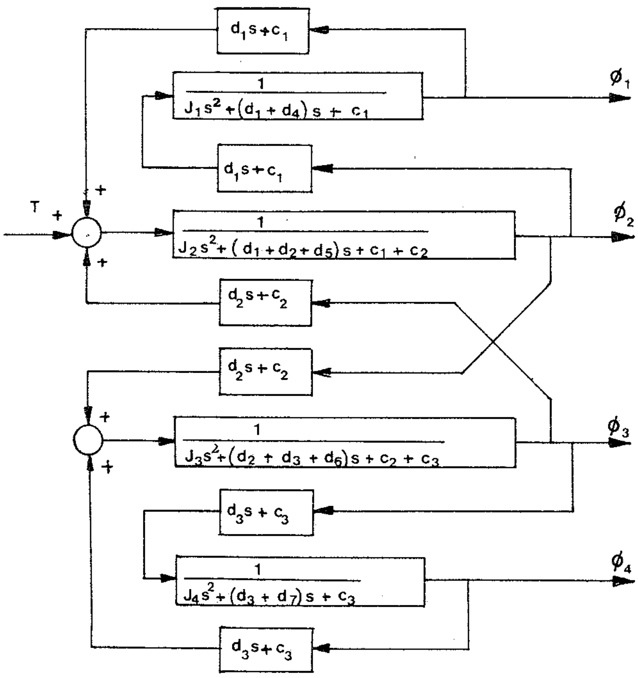

Fig. 7. Block diagram of the mechanical system

The connection of the motor and the mechanical system is shown in figure 8, where K_{Et} is the tachometer constant and block H represents the block diagram of figure 7.

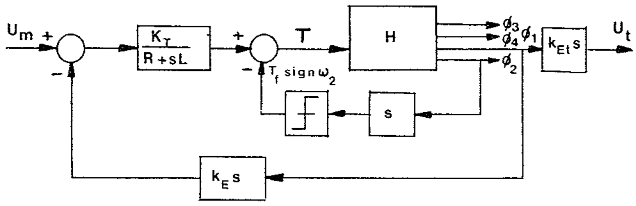

Fig. 8. Block diagram of the full model

Most of present day robot control systems are based on two feedback signals, namely the angular displacement and the angular velocity of the motor shaft. Through that, the harmonic-drive is out of the closed loop and so is the important nonlinearity backlash which commonly occurs in gear-box trains. Backlash is, in fact, the clearance between the teeth of the drive gear and those of the driven gear. By using the position of the load as a feedback signal, the backlash comes inside the closed loop and it influences the behaviour of the closed-loop system.
Dubrowsky and Freudenstein have shown that the "impact-pair" model (fig. 9) is a good starting unit for describing backlash.

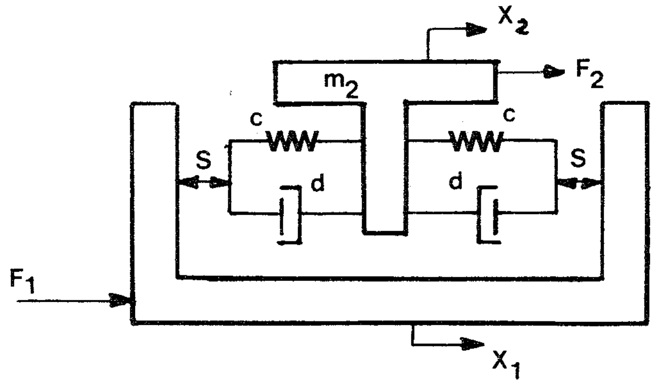

Fig. 9. "Impact-pair" model

In figure 9, F_1 and F_2 are forces, x_1 and x_2 are displacements; m_1 and m_2 are masses and S is the clearance. The equations of motion are :

– for $x_2 - x_1 < S \quad m_1\ddot x_1 = F_1 ; m_2\ddot x_2 = F_2.$ (18)

– for $x_2 - x_1 > S$

$$m_1\ddot x_1 = F_1 + c\,\{x_2 - x_1 - S\,\mathrm{sign}(x_2 - x_1)\} + d(\dot x_2 - \dot x_1) \tag{19a}$$

$$m_2\ddot x_2 = F_2 + c\,\{x_1 - x_2 - S\,\mathrm{sign}(x_1 - x_2)\} + d(\dot x_1 - \dot x_2) \tag{19b}$$

In the robot the clearance occurs between J_3 and J_4. The stiffness coefficient c and damping coefficient d are c_3 and d_3 respectively. The masses in the impact pair model must be replaced by J_3 and J_4.
Now, from figure 8 and the equations 14 to 19, the equations of motion of the overall model can be derived

$$L\dot{I}_m = U_m - RI_m - K_E\,\dot{\Phi}_2\,;\, U_t = K_{Et}\,\dot{\Phi}_1$$

$$J_1\ddot{\Phi}_1 = c_1\,(\Phi_2-\Phi_1) + d_1\,(\dot{\Phi}_2-\dot{\Phi}_1) - d_4\,\dot{\Phi}_1$$

$$J_2\,\ddot{\Phi}_2 = K_T I_m - T_f\,\text{sign}\,(\dot{\Phi}_2) + c_1(\Phi_1-\Phi_2) + d_1\,(\dot{\Phi}_1-\dot{\Phi}_2) - d_5\dot{\Phi}_2 + c_2(\Phi_3-\Phi_2)$$

As $|\Phi_4-\Phi_3| < S$

$$J_3\ddot{\Phi}_3 = c_2\,(\Phi_2-\Phi_3) + d_2(\dot{\Phi}_2-\dot{\Phi}_3) - d_6\,\dot{\Phi}_3$$

$$J_4\ddot{\Phi}_4 = -d_7\dot{\Phi}_4$$

As $|\Phi_4-\Phi_3| \geqslant S$

$$J_3\ddot{\Phi}_3 = c_2(\Phi_2-\Phi_3)+d_2(\dot{\Phi}_2-\dot{\Phi}_3)-d_6\dot{\Phi}_3+d_3\,(\dot{\Phi}_4-\dot{\Phi}_3) + c_3\,\{\Phi_4-\Phi_3-S\text{sign}\,(\Phi_4-\Phi_3)\}$$

$$J_4\ddot{\Phi}_4 = c_3\,\{\Phi_3-\Phi_4-S\text{sign}\,(\Phi_3-\Phi_4)\} + d_3(\dot{\Phi}_3-\dot{\Phi}_4)-d_7\dot{\Phi}_4$$

This model is of the 9th order and it contains 22 parameters and two nonlinearities. From the manuals of motor and harmonic-drive, a number of parameters are known and are included in the model. The other parameters could be estimated by direct and indirect measurements [7]. For one d.o.f. robot in accordance with the first d.o.f. of an ASEA IRb6 robot the results are :

$R=1{,}6\Omega$; $L=87\mu H$; $k_T=0{,}088Nm/A$; $k_E=0{,}088Vs/rad$; $k_{Et}=0{,}029Vs/rad$;

$T_f=0{,}025Nm$; $J_1=34$, $J_2=41$, $J_3=196$, $J_4=372$ (all. $10^{-6}kgm^2$);

$d_1=1200$, $d_2=68000$, $d_3=1600$, $d_4=76$, $d_5=12$, $d_6=700$, $d_7=0$ (all. $10^{-6}Nms/rad$);

$c_1=789$, $c_2=1225$, $c_3=1{,}44$ (all. Nm/rad).

Step responses of the model are obtained via simulation on a digital computer, using the simulation package PSI developed by the Delft University of Technology.
The frequency responses are calculated with a standard procedure based on an approximation of a set of complex linear equations by the Crout method of factorisation. With the use of a dynamic signal analyzer HP 5420A, the frequency response between U_t and U_m (fig. 8) of the real system was measured. A measurement and calculated response is given in figure 10.
Accompanying figure 10, the following remarks can be made. Mode 1 (16Hz) is due to the flexibility of the load-drive combination. Mode 2 (600Hz) comes predominantly from the motor-tachometer combination

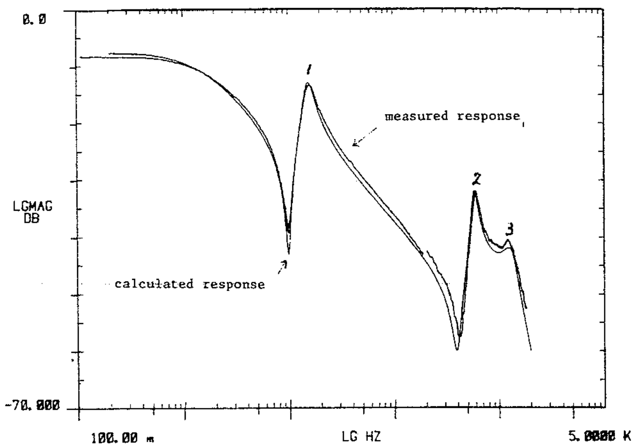

Fig. 10. Frequency responses of model and real system

and Mode 3(1200Hz) comes predominantly from the motor-drive combination.
The measuring shows that the assumption of rigid bodies is not allowed. The simulation result of the overall model indicates that the model is valid.
Figure 11 shows a step response.

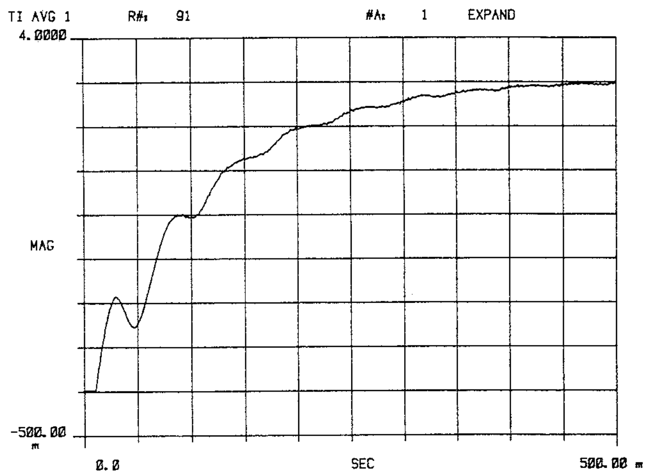

Fig. 11. Step response of the model

4.2. Sensitivity of the model to parameter variations

A model of a process will rarely contain the exact values of the process parameters. Therefore, the sensitivity of a model to parameter variations is of prime importance. For investigating model reduction, knowledge of the sensitivity to parameter variations is also important. Here we summarize the results of a parameter sensitivity analysis of the robot model. The results are obtained from the frequency responses by changing the model parameters one by one.
The inductance L has only influence on Mode 3. The damping coefficients d_1 and d_2 influence the amplitude of the frequency response over 500Hz, d_2 more than d_1. The stiffness coefficients c_1 and c_2 influence the high frequency behaviour, over 500 Hz. Mode 1 has strongly been influenced by d_3 (the amplitude of the frequency response only) and c_3 (figure 12).
The parameters J_4 and d_3 are slightly dependent. Variations of J_4 and d_3 have much influence on the low

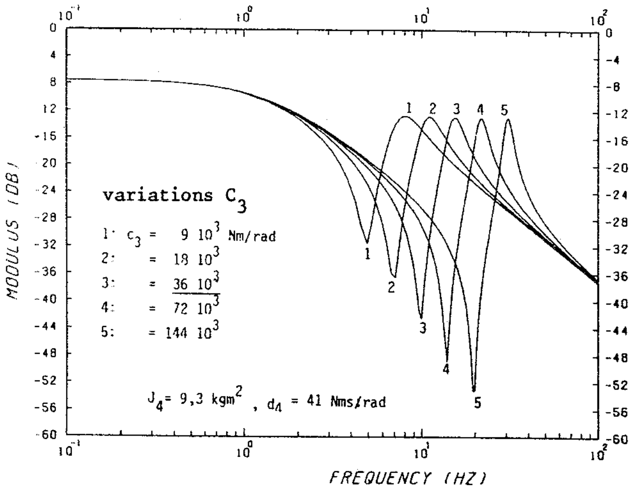

Fig. 12. Frequency responses, c_3 variable

frequency behaviour. The influence of the damping coefficients d_4, d_5, d_6 and d_7 on the system response is not very strong; and it makes no difference as the coefficients have been replaced by one equivalent motor damping coefficient $d_5^1 = d_4 + d_5 + d_6 + d_7$.

5. MODELLING A ROBOT WITH TWO DEGREES OF FREEDOM

The dynamical behaviour of an industrial robot with two d.o.f. is mainly determined by the description of the behaviour of the separate d.o.f. The parameters of the model describing this behaviour can become variables when more d.o.f. are added. The moment of inertia from the load is one of the most important variables. The parameters in the model which represent the torsion rigidity can also be variable (c_3 is load-dependent). A coupling between two links will always have a finite rigidity. Through this, extra torsion vibrations and bending phenomena may arise and these phenomena have to be introduced in the model.
The model of a non-rigid torsion coupling is rather simple. A fourth spring-damper combination has been introduced to the physical model of figure 6, between a part of the load, dependent on the connecting point, and the remaining elements of the load.
Modelling of the bending vibrations is not so easy because, apart from the moments of intertia, the masses of the coupled element are also of importance. However, these translations can also be modelled as mass-damper-spring systems. For each d.o.f., equation 11 becomes

$$K = \frac{1}{2}\sum_{i=1}^{4} J_i \dot{\Phi}_i^2 + \frac{1}{2}\sum_{i=1}^{4} m_i v_i^2$$

where : m_i = reduced mass on the desired distance calculated from J_i; v_i = velocity of the mass.

For the potential energy, the term $\frac{1}{2}\sum_{i=1}^{4} c_{bi} u_i^2$ must also be added, c_{bi} = bending stiffness and u_i = bending. Bending did not occur in the test set-up used.
This set-up is a copy of the first two d.o.f. of an ASEA IRb6 robot. So, the test robot consists of two links and two rotational joints. The first d.o.f. is a rotation on a perpendicular axis and the second d.o.f. is a rotation on an horizontal axis.
For any type of manipulator having rotational joints, the centripetal and coriolis forces can be of major importance in the dynamics. These forces introduce velocity-dependent nonlinearities. Further, the gravity forces may be important. In the model, these forces/torques can be interpreted as external forces/torques, but not all are equally important. Because the influences of the velocity-dependent forces are hard to measure on the test set-up, I am therefore restricted to some quantitative observations.
Following the Denavit-Hartenberg convention on the classification of the link, a centripetal force on point i as a result of its own speed is always zero. When making other choices of the coordinate system, the centripetal force as a result of its own speed is small in comparison to the stiffness links, so that bending does not occur.
If the joint is contained between one end of the two links (one-side-clasping), the centripetal torque on the second d.o.f. in consequence of rotation ω of the first d.o.f. is

$$T_{cf} = \frac{1}{8} m\, \omega^2 \ell^2 \sin 2\theta \qquad (20)$$

where : m = mass, ℓ = length and θ the angular displacement of the second arm. The quantity of the centripetal torque is dependent of the position of the second d.o.f.
The coriolis forces on joint i due to its own velocity can be interpreted as a viscous damping force. In the case of one-side-clasping of the arm the coriolis torque on the first d.o.f. due to the angular velocity $\dot{\theta}$ of the second d.o.f. is

$$T_{cor} = \frac{1}{8} m\, \dot{\Phi}\, \dot{\theta} \sin 2\theta \qquad (21)$$

where $\dot{\Phi}$ is the angular velocity of the first d.o.f.
The coriolis torque on the second d.o.f. is much smaller.
The gravity force on the first d.o.f. is not of importance, on account of the rotation around the vertical longitudinal axis. Again, in the case of one-side-clasping, the gravity torque on the second d.o.f. is given by

$$T_g = \frac{1}{2} m g \ell \sin\theta \qquad (22)$$

Since the equations 14 to 17 are valid for each d.o.f., equation 17 can be enlarged with the equations 20, 21 and 22.

$$J_{1,4}\ddot{\Phi}_4 = c_{1,3}(\Phi_3 - \Phi_4) + d_{1,3}(\dot{\Phi}_3 - \dot{\Phi}_4) - d_{1,7}\dot{\Phi}_4 - \frac{1}{8} m_2 \dot{\Phi}_4 \dot{\theta}_4 \sin 2\theta_4$$

$$J_{2,4}\ddot{\theta}_4 = c_{2,3}(\theta_3 - \theta_4) + d_{2,3}(\dot{\theta}_3 - \dot{\theta}_4) - d_{2,7}\dot{\theta}_4 + \frac{1}{2} m_2 g \ell_2 \sin\theta_4 + \frac{1}{8} m_2 \ell^2 \dot{\Phi}_4^2 \sin 2\theta_4$$

The index-numbers 1 and 2 refer to the first and second d.o.f. respectively. The gravity force produces an apparent change of the coefficients $c_{1,3}$ and $d_{1,3}$.

6. CONCLUSIONS

The trends in manipulator design has been to continually improve performance by increasing both precision and speed of motion. Simple kinematic and dynamic models based on the assumption that the links are to be considered as rigid-bodies are no longer adequate. The mechanical resonances in motor-load structure play a role if the resonance frequency becomes smaller than the required bandwidth of the beedback system. Both the mechanical system and control system require improved models for design simulation. In more realistic models, the elastic properties of mechanisms and nonlinearities in the actuator system should be taken into account.

A robot arm can be modelled as a mass-spring-damper system. The overall model of the robot consists of the model of the arm and the models of the actuator circuits. For one d.o.f. the model is of 9th order and contains 22 parameters and two nonlinearities.

Parameter sensitivity analysis shows that the dynamic behaviour of the robot is mainly determined by the coupling coefficients between the harmonic-drive and the load.

For robots with more than one d.o.f., the simulation time of the robot model is too long in on-line applications. This is due to the complexity of the model and the simulation of coulomb friction and backlash in the robot model. The simulation time might be reduced by the use of more advanced integration techniques.

REFERENCES

1. George Lee, C.S. : 'Robot Arm Kinematics, Dynamics and Control', IEEE Computer, December 1982, p. 62-79.
2. Luh, J. Y. S. : 'Conventional Controller Design for Industrial Robots – A Tutorial', IEEE Trans. on Systems, Man and Cybernetics, SMC-*13*, (3) May/June, p. 298-316 (1983).
3. Walker, M. W.; Orin, D. E. : 'Efficient Dynamic Computer Simulation of Robotic Mechanisms', Proc. 1981 Joint Automatic Control Conference, Charlottesville, Va., USA, 1981, WP-2B.
4. Luh, J. Y. S.; Walker, M. W.; Paul, R. P. C. : 'On-line Computation Scheme for Mechanical Manipulators', Journal of Dynamic Systems, Measurement and Control, *102*, June, p. 69-76 (1980).
5. Brussel, H. v.; Schutter, J de : 'Intelligent sensor-controlled robots', Journal A, *23*, (3), p. 133-142 (1982).
6. Machielsen, K. C. P. : 'Some Aspects of the Dynamic Behaviour of an Assembly Robot', M. Sc. Thesis, Measurement and Control Group, Dept. of Electrical Engineering, Eindhoven University of Technology, The Netherlands (1983).
7. Kruk, R. J. van der : 'The dynamic behaviour of an industrial robot with one degree of freedom' (in Dutch), M.Sc. Thesis, Measurement and Control Group, Dept. of Electrical Engineering, Eindhoven University of Technology, The Netherlands (1982).
8. Beljaars, J. W. F. M. : 'The dynamic behaviour of an industrial robot with two degrees of freedom' (in Dutch), M.Sc. Thesis, Measurement and Control Group, Dept. of Electrical Engineering, Eindhoven University of Technology, The Netherlands (1984).

H. H. VAN DE VEN graduated in 1959 in Electrical Engineering at the Delft University of Technology, the Netherlands. Since 1959 he has been employed in the EE-Department of the Eindhoven University of Technology, where he lectures in control and system theory. His research activities are dominantly in modelling and controlling of robotic manipulators.